Ultrastructure of Haustorium Development in *Puccinia coronata* f. sp. *avenae*: Cytochemistry and Energy Dispersive X-ray Analysis of the Haustorial Mother Cells

J. Chong and D. E. Harder

Agriculture Canada, Research Station, 195 Dafoe Road, Winnipeg, Manitoba, Canada R3T 2M9.
Based on a thesis submitted by the senior author for partial fulfillment of the requirements for a Ph.D. degree. We thank F. N. Ghadially and N. K. Yong, Department of Pathology, University Hospital, University of Saskatchewan, Canada, for the EDX facilities. The technical assistance of K. Shewchuk is gratefully acknowledged.
Contribution 1022 from Agriculture Canada, Research Station, Winnipeg, Manitoba, Canada.
Accepted for publication 5 May 1982.

ABSTRACT

Chong, J., and Harder, D. E. 1982. Ultrastructure of haustorium development in *Puccinia coronata* f. sp. *avenae*: Cytochemistry and energy dispersive X-ray analysis of the haustorial mother cells. Phytopathology 72:1518-1526.

In young haustorial mother cells (HMCs) of *Puccinia coronata* f. sp. *avenae* all of the mitochondria were arranged around the periphery of the protoplast. With uranyl acetate and lead citrate staining, five HMC wall layers were resolved compared to two in the hyphal walls. With periodic acid-thiocarbohydrazide-silver proteinate staining, three layers were observed in the HMC walls, but only one layer in the hyphal walls. The HMC septa contained more layers than did septa in the mycelial hyphae. All mycelial walls and septa were shown to contain protein, lipid, and polysaccharide components. Energy dispersive X-ray (EDX) analysis revealed silicon deposits in the walls of many HMCs, including their septa, located at or near the centers of the infection colonies. Haustorial mother cells with heavy silicification were often collapsed, and were associated with aberrant haustoria. Phosphorus-rich iron and sulphur-containing deposits were commonly detected by EDX analysis in the protoplasts of HMCs and older haustoria.

Additional key words: *Avena sativa*, protease, cellulase, ether/ethanol, acetone, chloroform/methanol extraction.

The structural aspects of haustoria and their relationship with their hosts have been quite well characterized (5,24). However, less attention has been paid to the fine structural features and details of the ontogeny of the haustorial mother cells (HMCs) from which the haustoria are differentiated. Perhaps this lack of information is due to the difficulty of predicting whether a particular hyphal tip is an incipient HMC. Results of previous studies of haustorium ontogeny (10,19) show characteristic long membrane protrusions that develop on the hyphal side of the HMC septum during early haustorium formation. The presence of these long membrane protrusions is an accurate indicator of a young HMC. In *Uromyces phaseoli* var. *vignae*, the septum that delimits the HMC from the rest of the mycelium has also been shown to be structurally distinct from hyphal septa elsewhere in the mycelium (19).

The purpose of this study was to describe in detail the ultrastructure of the HMCs and hyphal cells of *Puccinia coronata* Cda. f. sp. *avenae* Eriks. Various cytochemical methods and energy dispersive X-ray (EDX) analysis were also applied to compare the composition of these structures with that of other parts of the haustorial apparatus (9,10). The significance of these results is discussed in relation to HMC function and to their probable mode of differentiation from the hyphal cells.

MATERIALS AND METHODS

Plant material and inoculation. Seedlings of *Avena sativa* L. 'Pendek' were grown and inoculated with urediospores of a compatible race (race 326) of *P. coronata avenae* as outlined previously (9).

Conventional fixing and staining for electron microscopy. Developing rust colonies were sampled at various times beginning 5 days after inoculation. The excised infected tissue was fixed with glutaraldehyde, then either postfixed with osmium tetroxide (OsO_4) or processed further without OsO_4 postfixation (9). Ultrathin sections were cut from near the edge and center of the infection colonies, mounted on formvar- and carbon-coated 149-μm (100-mesh) or single-hole copper grids, stained with uranyl acetate and lead citrate (UA/PbC), and examined with a Hitachi HU-12 electron microscope.

Thiéry periodic acid-thiocarbohydrazide-silver proteinate staining. Periodate oxidation (26), staining, and control treatments (11,12) for the Thiéry staining method (33) have been described (9).

Solvent extractions and enzyme treatments. Infected tissue fixed with glutaraldehyde was subjected to organic solvent extraction (ether/ethanol, acetone, or chloroform/methanol) or enzyme treatment before postfixation with OsO_4 as described previously (10,21). The enzymes were: protease (Sigma, type V, purified, 1–5 mg/ml in 0.05M tris-HCl buffer, pH 7.5), cellulase (Sigma, type I, practical grade, 5 mg/ml in 0.05 M phosphate buffer, pH 5.5). Ultrathin sections of specimens treated with organic solvents or enzymes were poststained with UA/PbC, or the Thiéry staining procedure as described above.

Energy dispersive X-ray analysis. Glutaraldehyde-fixed, unosmicated, infected leaf tissue, processed as described above, was used for X-ray analysis. Microtome sections with a thickness giving a blue interference color were mounted on formvar- and carbon coated 149-μm (100-mesh) copper grids. Energy dispersive X-ray analysis of unstained sections was carried out by using a Philips EM-400 transmission electron microscope to which was connected a computerized energy dispersive X-ray analysis (Edax-Edit, Edax International, Prairie View, IL 60069) unit. When the target (area containing electron-opaque deposits) was located, the electron beam was reduced to a spot size of about 0.2 μm and aligned to focus on the target. Counts of X-ray pulses were then collected for a period of 100 sec live time. The spectrum thus obtained was displayed on a cathode-ray screen and photographed. To obtain control data, spectra were similarly obtained from an area adjacent to the target. All X-ray analyses were carried out at an acceleration voltage of 60 kV.

The publication costs of this article were defrayed in part by page charge payment. This article must therefore be hereby marked "*advertisement*" in accordance with 18 U.S.C. § 1734 solely to indicate this fact.

RESULTS

HMC protoplasts. The cytoplasmic contents of young HMCs were generally similar to those of intercellular hyphal cells in terms of nuclei, mitochondria, endoplasmic reticulum, glycogen granules, and lipid droplets. There were small vacuoles (Figs. 1 and 2) which frequently contained electron-opaque deposits (Fig. 3). The nature of the electron-opaque deposits will be discussed in a later section.

A characteristic feature of HMCs was that the mitochondria were compact and were located around the periphery of the cell, adjacent to the plasmalemma (Figs. 1 and 2). They were never found near the center of the cell protoplast. In cross sections, a similar pattern of mitochondrion distribution was observed, and the mitochondria appeared as a ring around the periphery of the protoplast (Fig. 4). In hyphal cells, the mitochondria were

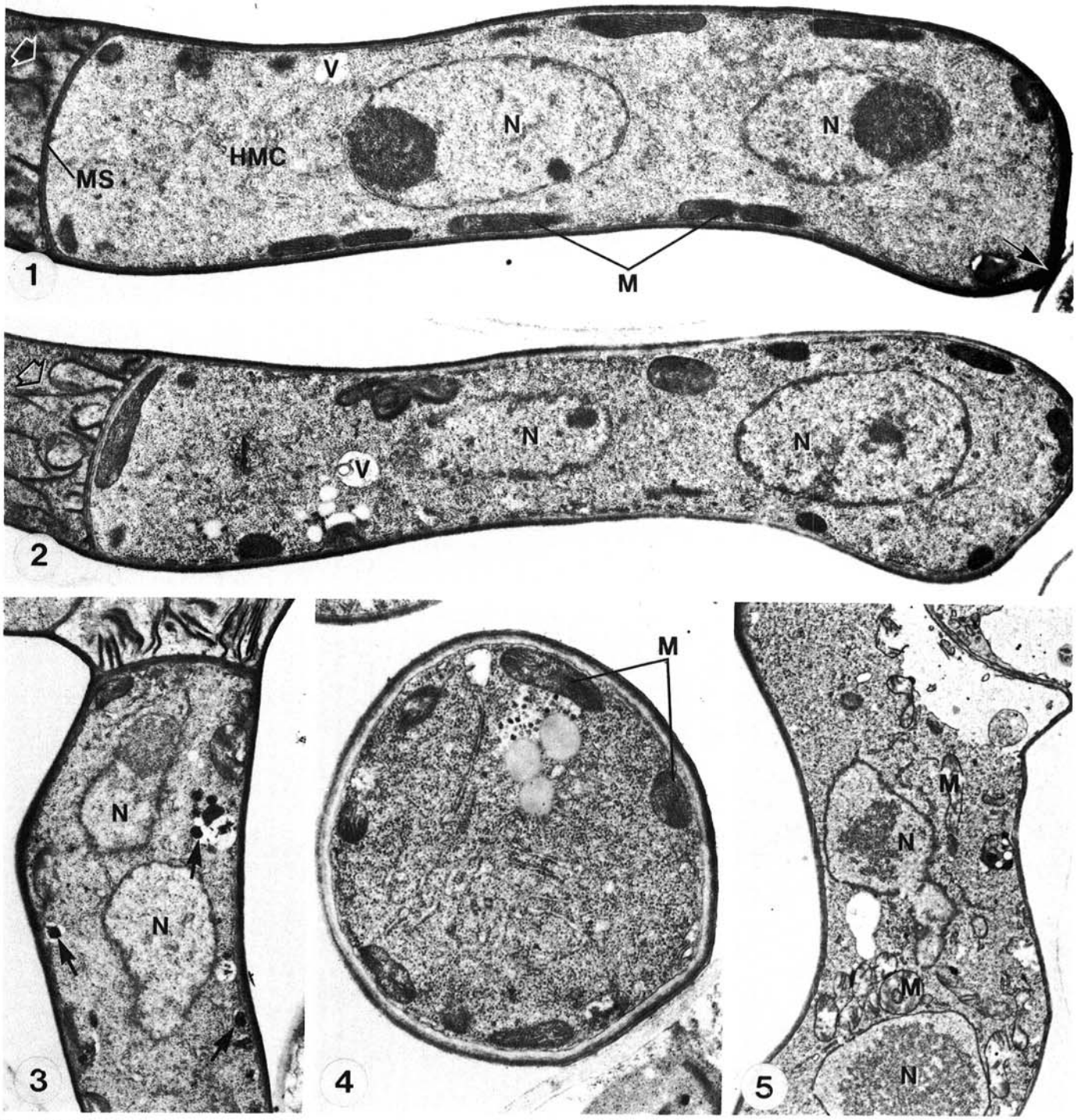

Figs. 1–5. Ultrathin sections of *Puccinia coronata avenae*. Abbreviations: Glt, glutaraldehyde; HMC, haustorial mother cell; M, mitochondrion; MS, haustorial mother cell septum; N, nucleus; OsO_4, osmium tetroxide; PbC, lead citrate; UA, uranyl acetate; and V, vacuole. **1 and 2.** Two closely adjacent sections taken from a series of serial sections of the same young HMC. Host wall penetration had begun (arrow), but the haustorium had not yet formed. Mitochondria are densely stained and located around the periphery adjacent to the plasmalemma. The protoplast contains two nuclei, small vacuoles, and an abundance of ribosomes. The relatively young age of the HMC is also indicated by the presence of long membrane protrusions on the hyphal side of the HMC septum (open arrow). Glt/OsO_4. UA/PbC. **1,** × 15,400. **2,** × 14,600. **3,** Electron-opaque deposits (arrows) in small vacuoles of a young HMC. Glt/OsO_4. UA/Pbc. × 14,900. **4,** Cross section of a young HMC with mitochondria arranged as a ring around the periphery of the cell adjacent to the plasmalemma. Glt/OsO_4. UA/PbC. × 23,100. **5,** Part of a hyphal cell with mitochondria scattered at random locations in the cell protoplast. Glt/OsO_4. UA/PbC. × 10,600.

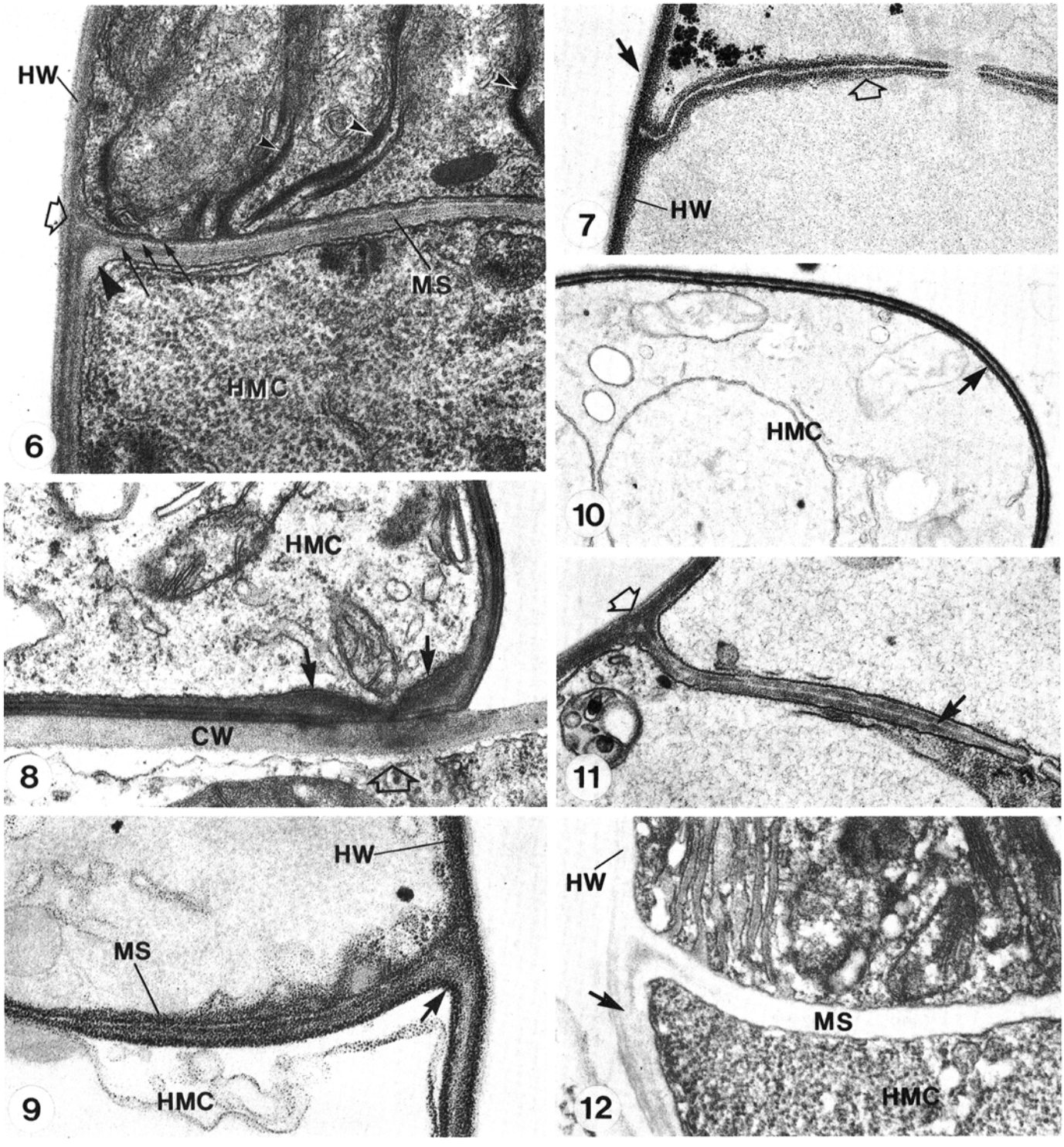

Figs. 6–12. Ultrathin sections of *Puccinia coronata avenae* showing different wall structure and properties revealed by different staining techniques. Abbreviations: CW, host wall; Glt, glutaraldehyde; HMC, haustorial mother cell; HW, hyphal wall; MS, haustorial mother cell septum; N, nucleus; OsO_4, osmium tetroxide; PA-TCH-SP, periodic acid-thiocarbohydrazide-silver proteinate; PbC, lead citrate; and UA, uranyl acetate. **6,** A section showing part of a HMC septum (MS) which is composed of four layers. The two electron-opaque layers (long arrows) are continuous with the periclinal wall (open arrow). A third, more lightly stained layer (short arrow) separates the two electron-opaque layers and ends at the periclinal wall. The fourth lightly stained layer (large arrowhead) is continuous around the rest of the HMC. The HMC wall is composed of five layers and is thicker than the hyphal wall which has only two layers. Note the long membrane protrusions (small arrowheads) on the hyphal side of the HMC septum. Glt/OsO_4. UA/PbC. × 44,300. **7,** The hyphal wall is composed of one densely staining layer excluding the lightly stained layer of extracellular substance (arrow). The hyphal septum (open arrow) consists of two electron-opaque layers separated by a middle electron-lucent layer which ends at the periclinal wall. Glt/OsO_4. PA-TCH-SP. × 48,600. **8,** An HMC sectioned near the site of host penetration (open arrow). The HMC wall is composed of five layers except at the region of host penetration (arrows). Glt/OsO_4. UA/PbC. × 36,400. **9,** The HMC septum is multilayered. Three layers are observed in the HMC wall: two electron-opaque layers separated by a middle moderately stained layer. The innermost electron-opaque layer is continuous around the septum (arrow). Glt/OsO_4. PA-TCH-SP. × 60,700. **10,** The HMC wall (arrow) contains three layers: two electron-opaque layers separated by a moderately staining middle layer. Glt/OsO_4. PA-TCH-SP. ×19,400. **11,** Part of a hyphal septum (arrow) showing two electron-opaque layers separated by a narrow electron-lucent central lamella which ends at the periclinal wall (open arrow). The two electron-opaque layers are continuous with the periclinal wall. Glt/OsO_4. UA/PbC. × 41,000. **12,** The HMC wall (arrow) and septum are lighter stained after lipid-solvent extraction as compared to the untreated ones shown in Fig. 6. Glt-acetone-OsO_4. UA/PbC. ×46,400.

scattered, frequently in small groups, at various locations in the protoplasts (Fig. 5).

Cell walls and septa. The HMCs could be distinguished from intercellular hyphal cells by differences in wall structure as revealed by different staining methods. With UA/PbC staining of intercellular hyphal cells, two wall layers were differentiated (Fig. 6), while the Thiéry method revealed only one electron-opaque layer, excluding a lightly-stained layer of extracellular substance (Fig. 7). In contrast, the HMC walls were thicker and five wall layers were visible with UA/PbC staining: three moderately stained layers were separated by two electron-opaque layers (Figs. 6 and 8). With the Thiéry staining method, three wall layers in the HMC walls were resolved: two electron-opaque layers separated by a moderately stained layer (Figs. 9 and 10).

The HMC septum also differed structurally from the septa found elsewhere in the mycelium. With UA/PbC staining, four layers were visible in the HMC septum (Fig. 6). Of the four layers two were electron-opaque; these were separated by a third more lightly stained layer. The fourth layer stained similarly in intensity to the third layer and was found adjacent to the fungal plasmalemma on the HMC side of the septum. The third layer ended at the periclinal wall, while the electron-opaque layers were continuous with it. The fourth layer that was located adjacent to the HMC plasmalemma was continuous around the rest of the HMC (Fig. 6). In all septa elsewhere in the hyphae, only three layers were observed with UA/PbC staining: two electron-opaque layers separated by a narrow electron-lucent central lamella that ended at the periclinal wall (Fig. 11). The two electron-opaque layers were continuous with the periclinal walls. With the Thiéry staining method three layers were also found in the hyphal septum (Fig. 7) but the HMC septum was observed to contain as many as six layers (Fig. 9).

The fungal walls and septa remained unstained in all control treatments for the Thiéry procedure which indicates that these structures contain polysaccharides with vicinal hydroxyl groups (11,12). However, certain groups of fatty acids and polypeptides also react to periodic acid oxidation and are stained with the Thiéry procedure (14,16). To ascertain this possibility, infected leaf tissue was treated with lipid solvents or protease. After lipid solvent treatment, the lipid-containing chloroplast plastoglobuli (normally seen as electron-opaque globules in UA/Pb stained sections of unextracted tissue) became electron-lucent, indicating that lipid had been extracted. In fungal walls and septa, there was a large reduction in staining intensity by UA/PbC after solvent treatment (Fig. 12). The staining of these structures by using the Thiéry procedure however, was not affected by the solvent treatment. After protease treatment, marked erosion was observed in both fungal and host cytoplasm, while host walls appeared to be little affected. Structural integrity of the chloroplasts was markedly affected, and the stroma was extensively extracted, but the plastoglobuli remained unchanged and showed no loss in staining intensity. Some extraction apparently occurred in the fungal walls, as they appeared more fibrillar and less discrete in outline than the untreated ones, and their usual layered appearance was lacking (Fig. 13). Staining of these walls with the Thiéry procedure however, was not affected after protease treatment.

Cellulose, a β-1,4-glucan, is known to be a component in some fungal walls (4). It contains vicinal glycols and is also stained by the Thiéry procedure (Fig. 14). Treatment of glutaraldehyde-fixed specimens with cellulase resulted in the removal of material from host walls (Fig. 15), but the treatment did not affect fungal walls or septa.

HMCs at or near the center of the infection colonies. In the present study, unique structural changes were observed in the walls and septa of many of the HMCs found at or near the centers of the colonies. In sections of glutaraldehyde/OsO_4-fixed tissues and after staining with UA/PbC, electron-opaque deposits were located in the walls and septa of these HMCs. Examples are shown in Figs. 16 and 17. These deposits formed a dense layer inside the walls and septa of the HMCs, except for a small portion of the septum around the septal pore (Fig. 16). In the thickened wall region of the HMCs at the penetration site the deposits appeared as large, electron-opaque granules (Fig. 17). Aberrant haustoria were frequently found at or near the centers of the colonies (Fig. 18) and many of these haustoria were associated with those HMCs that had heavy wall deposit (Fig. 19). Similar electron-opaque deposits were not observed in the septa or in the walls of the HMCs located at or near the edge of the same colonies. The appearance of the deposits in the above structures found at or near the centers of the colonies was more common in older colonies than in those sampled at 5 days after inoculation.

Near the centers of the colonies, some hyphal tips still differentiated to form HMCs. In the earliest stage of deposition that could be detected, the electron-opaque deposits were found in the membrane protrusions (Fig. 20), but not in the walls and septa of these young HMCs. These deposits were prominent in unstained sections (Fig. 21). After haustorium formation, but prior to nuclear migration, granular electron-opaque deposits appeared in the thickened portion of the HMC wall at the site of host cell penetration (Fig. 22). At about this time or shortly after, granular deposits were found in the HMC septum and in the rest of the wall around the HMC. More deposits then appeared in the membrane protrusions and in the HMC walls and septa (Fig. 23). In apparently later stages of development the walls of the HMCs were completely impregnated with these deposits, and the cells collapsed.

The electron-opaque deposits in the above structures were resistant to lipid solvent extraction, protease digestion, and periodic acid treatment (Fig. 22). Since these deposits were electron-opaque in unstained sections of glutaraldehyde fixed, unosmicated materials (Figs. 21 and 23), they were subjected to EDX analysis.

A 7-day-old colony was chosen for EDX analysis of the electron-opaque deposits. Sections were taken from various areas of the colony to obtain HMCs undergoing various stages of development. Stages showing the initial deposition of electron-opaque deposits in the membrane protrusions and in the thickened portion of the HMC at the site of host penetration, as well as the subsequent heavy accumulation of the deposits in the rest of the HMC wall and septum, were located readily within or near the center of the colony. A number of analyses were made on these structures, but only one example will be presented. For comparison, membrane protrusions, HMC walls and septa found at the edge of the colony, and other mycelial walls that were free of any electron-opaque deposits were also analyzed.

Where electron-opaque deposits appeared inside the membrane protrusions (Fig. 21), silicon was the major element present (Fig. 27). The peak representing copper was assumed to have originated from the copper support grid. To show that the silicon peak was significant, the hyphal wall adjacent to the above membrane protrusion was also analyzed. This revealed only a small peak of silicon (Fig. 28). Analysis of the formvar-carbon support film also showed trace amounts of silicon (Fig. 29), which could account for the small amounts of silicon detected in the analysis of the hyphal wall. Thus, our tests demonstrated that silicon was a major element present in the electron-opaque deposits.

At the site of host penetration (Fig. 22) EDX analysis of the electron-opaque deposits in the thickened portion of the HMC wall indicated that silicon was also the major element in these deposits. With older HMCs, EDX analysis similarly revealed a major silicon peak in the electron-opaque wall and septum. Silicon was therefore also a prominent element in this modified HMC wall and septum. In contrast, no silicon was detected in significant amounts in the walls and septal structures of the younger HMCs, that were located near the edge of the colony.

To determine the possible source of silicon in the HMCs, air-dried ungerminated urediospores were subjected to EDX analysis. No significant amounts of silicon could be detected on the wall surface of the urediospores. Also, no electron-opaque deposits were observed in unstained sections of the urediospores fixed in gluataraldehyde alone.

During the course of the present EDX analysis, large electron-opaque deposits were detected in the cytoplasm of HMCs (Fig. 24) and older haustoria (Fig. 25) in unstained sections of glutarldehyde-fixed, unosmicated tissue. Spectra of these deposits

found in the HMCs and haustoria revealed that they were similar in composition. An example is shown in Figure 30. These deposits contained a high concentration of phosphorus, with small amounts of iron and sulphur. In stained sections of glutaraldehyde/OsO_4-fixed tissue electron-opaque deposits were also commonly found in vacuoles of hyphal cells (Fig. 26).

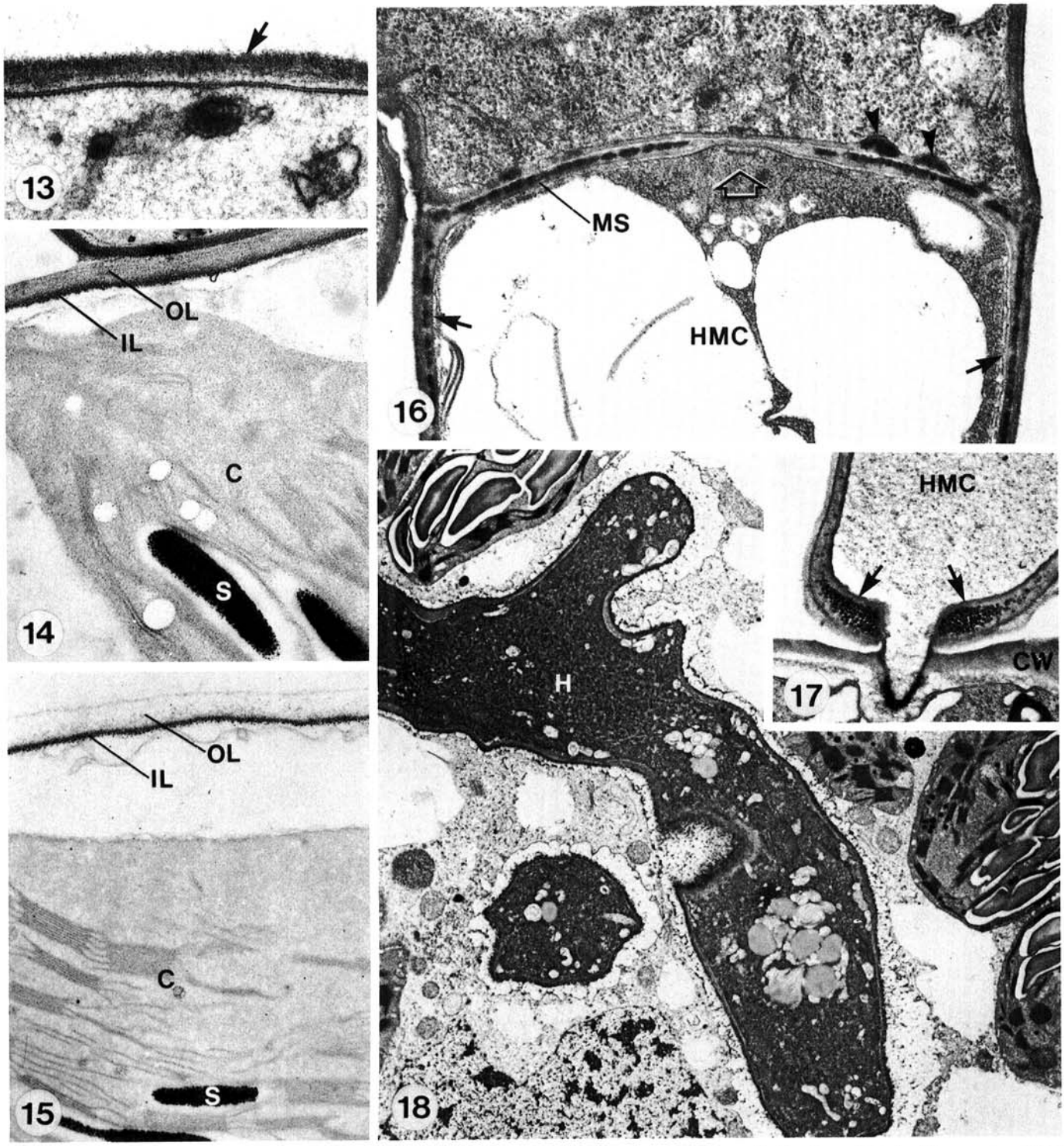

Figs. 13–18. Ultrathin sections of *Puccinia coronata avenae* in oats. Abbreviations: C, chloroplast; CW, host wall; Glt, glutaraldehyde; H, haustorium; HMC, haustorial mother cell; IL, inner layer; MS, haustorial mother cell septum; OL, outer layer; OsO_4, osmium tetroxide; PA-TCH-SP, periodic acid-thiocarbohydrazide-silver proteinate; PbC, lead citrate; S, starch granules; and UA, uranyl acetate. **13,** The HMC wall (arrow) is more fibrillar and less discrete in appearance after protease treatment than the untreated ones shown in Fig. 8. Glt-protease-OsO_4. UA/PbC. × 66,400. **14,** Thiéry staining of starch granules in a chloroplast. The host wall is seen as two layers: the outer layer is more lightly stained than the inner layer. Glt/OsO_4. PA-TCH-SP. × 33,200. **15,** The outer layer of the host wall is largely electron-lucent after cellulase treatment. Inner layer of the host wall and starch granules were unaffected. Glt-cellulase-OsO_4. PA-TCH-SP. × 27,900. **16,** A near median section of a HMC located near the center of an infection colony. Electron-opaque deposits are found inside the membrane protrusions (arrowheads), HMC septum and wall (arrows). A portion of the HMC septum around the septal pore region (open arrow) is free of these deposits. Glt/OsO_4. UA/PbC. × 40,000. **17,** An oblique section through the penetration region of the host cell wall. Granular electron-opaque deposits are found at the thickened region (arrows) of the HMC wall. Glt/OsO_4. UA/PbC. × 23,600. **18,** An aberrant haustorium with electron-dense cytoplasm and irregular outline in a host cell located near the center of an infection colony. Glt/OsO_4. UA/PbC. × 8,000.

DISCUSSION

Once the HMC septa were formed, the HMCs of *P. coronata avenae* were easily distinguished from the other hyphal cells by the distinctive pattern of mitochondrion distribution in the HMC protoplasts and differences in the number of wall layers observed in the HMC and hyphal cell walls. The HMC septa also contained more layers than did septa elsewhere in the mycelium. The above observations indicate that the HMC of *P. coronata avenae* is structurally more specialized than the intercellular hyphal cells.

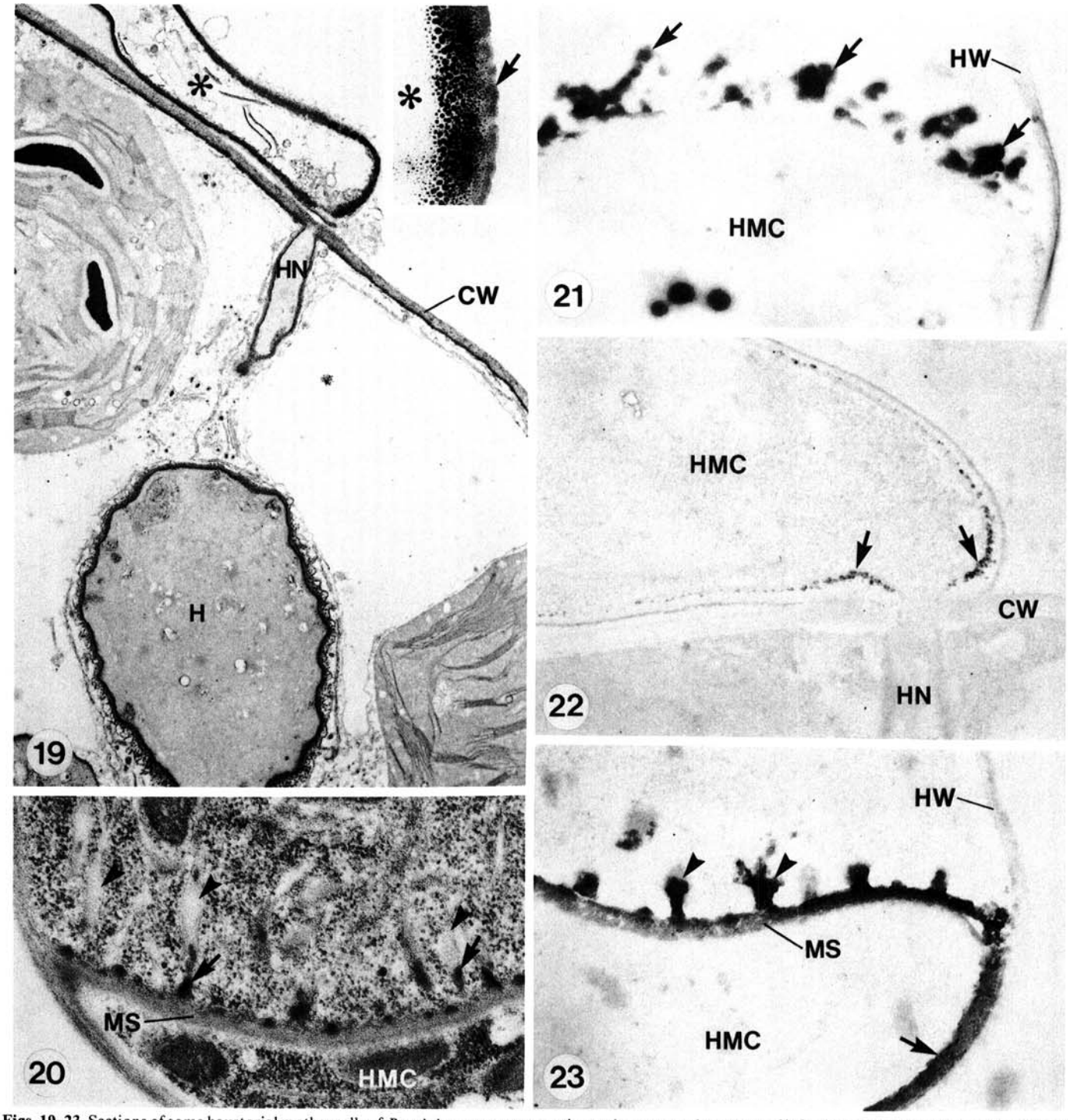

Figs. 19–23. Sections of some haustorial mother cells of *Puccinia coronata avenae* located at or near the centers of infection colonies in oats. Abbreviations: CW, host wall; Glt, glutaraldehyde; H, haustorium; HMC, haustorial mother cell; HN, haustorial neck; HW, hyphal wall; MS, haustorial mother cell septum; OsO_4, osmium tetroxide; PA-TCH-SP, periodic acid-thiocarbohydrazide-silver proteinate; PbC, lead citrate; UA, uranyl acetate. **19,** A necrotic haustorium associated with an empty and abnormally shaped HMC (asterisk). The inset shows a higher magnification of the HMC wall. Electron-opaque deposits (arrow) normally not found in healthy HMC walls, are found in the wall of this HMC. These deposits can be differentiated from the coarsely granular HMC wall stained by the Thiéry method. Glt/OsO_4. PA-TCH-SP. × 14,200. Inset. ×72,900. **20,** Electron-opaque deposits found inside membrane protrusions are indicated by arrows. The rest of the matrix (arrowheads) is largely electron-lucent. The HMC wall and septum are free of electron-opaque deposits at this stage. Glt. UA/PbC. × 37,500. **21,** A semithin (blue interference color) section of the membrane protrusions with electron-opaque deposits (arrows). This section had been subjected to energy dispersive X-ray analysis and the spectrum is shown in Fig. 27. Glt. Unstained section. × 18,600. **22,** Electron-opaque deposits (arrows) accumulated mainly in the thickened region of the HMC wall at the site of host penetration. Glt/OsO_4. This section had been treated with 1% periodic acid for 30 min, and was not stained. × 32,100. **23,** Heavy accumulation of electron-opaque deposits in the membrane protrusions (arrowheads), HMC septum and wall (arrow). This HMC had collapsed. Glt. Unstained section. ×46,400.

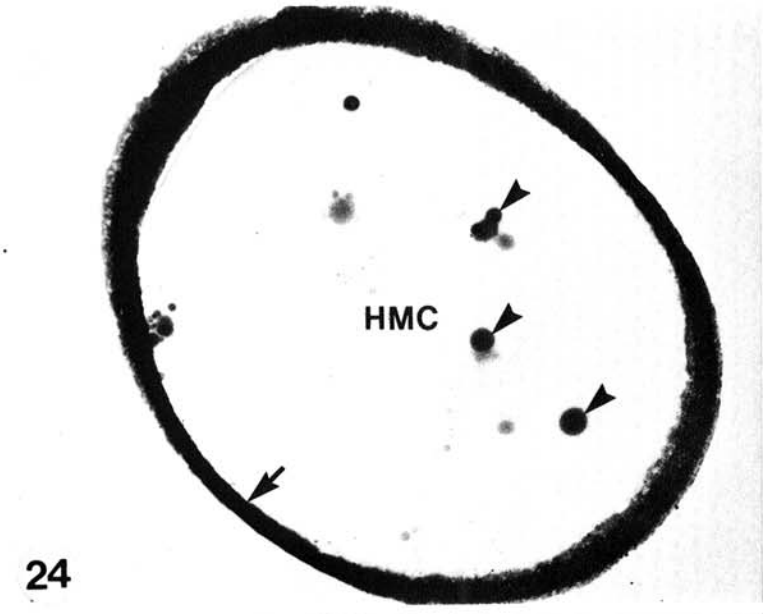

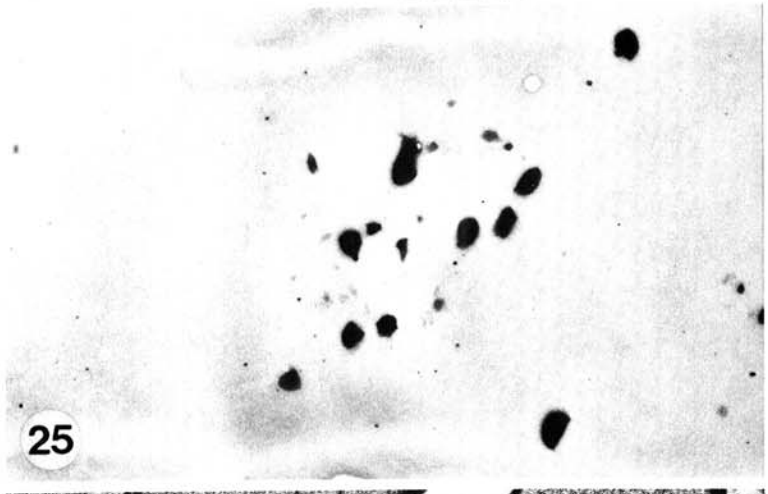

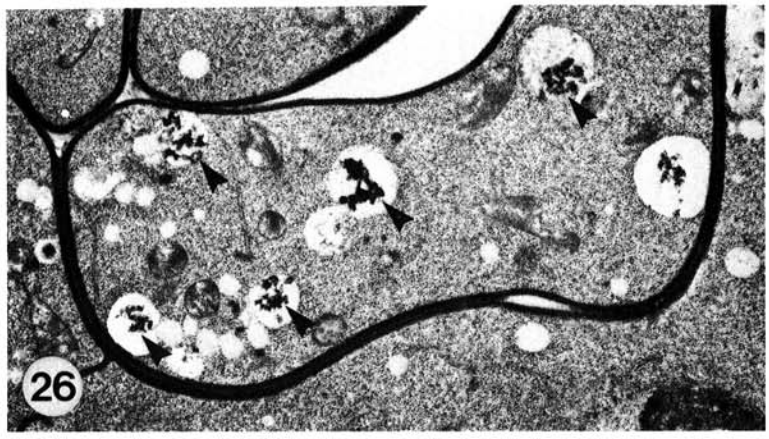

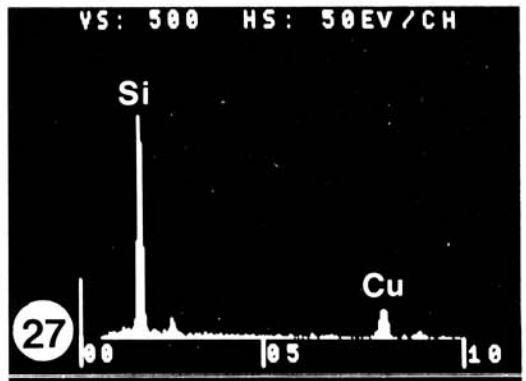

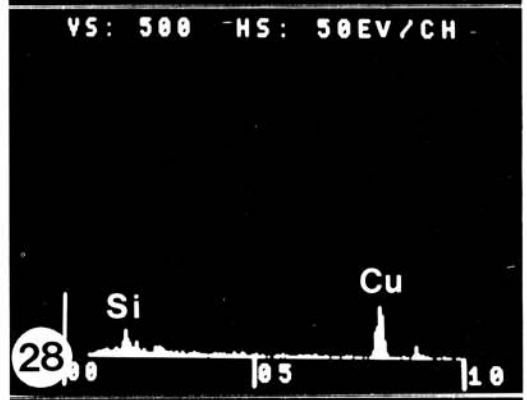

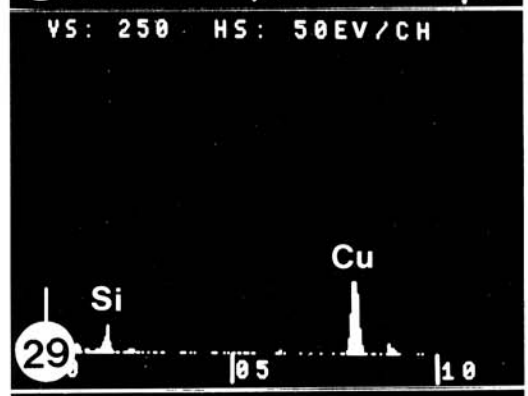

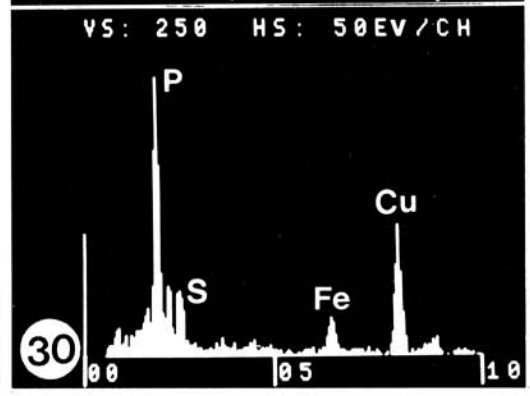

Figs. 24–30. 24–26, Sections of *Puccinia coronata avenae* in oats. **27–30,** Energy dispersive X-ray (EDX) spectra. Abbreviations: Glt, glutaraldehyde; HMC, haustorial mother cell; OsO_4, osmium tetroxide; PbC, lead citrate; UA, uranyl acetate. **24,** A semithin (blue interference color) cross section of an old HMC with heavy accumulation of electron-opaque deposits in its wall (arrow). Round electron-opaque deposits (arrowheads) are found in the vacuole. This section had been subjected to EDX analysis, and the spectrum is shown in Fig. 30. Glt. Unstained section. ×30,000. **25,** A semithin (blue interference color) section of part of an old haustorium. Electron-opaque deposits are found in the protoplast. Glt. Unstained section. × 17,100. **26,** Electron-opaque deposits (arrowheads) found in vacuoles of a hyphal cell in the sporogenous tissue. Glt/OsO_4. UA/PbC. ×12,100. **27,** EDX spectrum of the electron-opaque deposits in the membrane protrusions in Fig. 21. Silicon is the major element present. The peak representing copper in this spectrum and in the following spectra is assumed to have originated from the copper support grid. **28,** EDX spectrum of the hyphal wall adjacent to the membrane protrusions shown in Fig. 21. Only a small peak of silicon was detected, the amounts of which can be accounted for in the control analysis of the formvar-carbon support film shown in Fig. 29. **29,** EDX spectrum from an area of the formvar-carbon support film on a copper grid free of any sections of tissue. There were silicon and copper present in amounts sufficient to account for the silicon in the control analysis of the hyphal wall, and for the copper in all analyses. **30,** EDX spectrum of the vacuolar electron-opaque deposits in an old HMC shown in Fig. 24. Phosphorus was detected as the major element present, with small amounts of iron and sulphur.

Differences in the number of wall layers in the HMC and hyphal cell walls have also been reported in *U. phaseoli vignae* (19) and in *P. graminis tritici* (8). With the latter fungus, the distribution of the mitochondria in the protoplasts of young HMCs (8) was also shown to be similar to that in *P. coronata avenae*. However, there is insufficient information in the literature to determine if a similar distribution of mitochondria is general in the HMCs of the rust fungi.

In light microscopy studies Allen (1) and Ruttle and Fraser (28) observed that certain hyphal tips that were about to form HMCs became swollen with their ends closely appressed to the host cell walls. The induction of HMC differentiation thus appears to occur prior to HMC septum formation. Results of the present study further showed that walls of HMCs contained more layers than did other hyphal walls. This suggests that HMC specialization begins with additional wall layers, and the HMC is not merely formed by septation of a hyphal tip.

Cytochemically all mycelial walls and septa were shown to be similar in composition. They were intensely stained with the Thiéry procedure. This staining was not affected after protease or lipid solvent treatment, suggesting that the positive Thiéry staining of the fungal walls and septa in the untreated tissue was not due to protein or lipid. The staining of the fungal walls and septa by the Thiéry procedure and results of the control treatments therefore conform to what would be expected for structures containing polysaccharides with vicinal hydroxyl groups (11,12). Nevertheless, the loss of UA/PbC staining in these walls and septa after lipid solvent treatment suggests that they also contain lipid. The fact that all mycelial walls and septa became more fibrillar in appearance and lacked a layered structure after protease treatment indicated that protein was also present as a component.

In a previous study on *P. coronata avenae* in which the colloidal gold-lectin binding method was used, all mycelial walls and septa were also shown to contain wheat germ lectin and Conconavalin A (Con A) receptor sites (10). The binding of wheat germ lectin to these structures was concluded to be due to *N*-acetyl-glucosamine-containing receptors, indicating the presence of chitin. With Con A, however, it was not certain whether the binding was due to glucan and/or mannan. Glucans are known to be common wall constituents of many fungi (2,22) and those with vicinal glycols are stained by the Thiéry procedure. Further investigations are needed to determine the specific types of polysaccharides present in the mycelial walls and septa of *P. coronata avenae*.

In the present study, electron-opaque deposits were found in the walls and septa of many of the HMCs of *P. coronata avenae* located at or near the centers of the infection colonies. These deposits were shown by EDX analysis to contain silicon. Similar electron-opaque deposits were also found in the walls and septa of many of the HMCs of *P. graminis tritici* located at or near the centers of the colonies (8) and in the walls of some HMCs found in the nonhost reactions with *U. phaseoli vignae* (17). However, the nature of the deposits in these latter fungi had not been determined. Changes in wall appearance of the HMCs located in the central regions of older colonies were also observed in *P. coronata avenae* (28) and *P. graminis tritici* (1) by light microscopy. These HMCs were distorted and the appearance of their walls was described as glassy and swollen. In extreme cases, the lumen of the HMC was almost obliterated. The haustoria associated with these HMCs were also abnormal in appearance. Results of the present study supplemented these findings. The silicon deposits that were frequently found in the walls and septa of many HMCs of *P. coronata avenae* located mainly in the center of the colonies may be responsible for the "glassy" appearance observed by light microscopy. Further, the HMCs showing heavy silicification in their walls were often collapsed and frequently they were found to be associated with aberrant, necrotic haustoria which were common in host cells at the centers of older colonies. Necrosis of haustoria in these host cells indicates incompatibility, which probably resulted from the production of deleterious cell breakdown products. Samborski et al (29) observed necrotic host cells near the centers of otherwise vigorous compatible colonies in the wheat/stem rust system; it was suggested that this resulted from a general stress reaction. It has been discussed previously that the silicon deposits found in the neck ring of *P. coronata avenae* could very well function as a form of permeability barrier (9). It is possible that the heavy silicification seen in the HMC walls and septa is a protective mechanism of the fungus and acts as a form of permeability barrier to prevent or minimize the passage of deleterious cell-breakdown products to the rest of the mycelium.

The finding of silicon in *P. coronata avenae* appears to be unique among the rust fungi so far described. As discussed previously (9), silicon is rarely found in fungi, but it is a common constituent of plant tissue, particularly in gramineaceous plants including oats. It appears that the silicon in the HMC walls and septa originated from the host plant because silicon was not found in the urediospores. Assuming that a source of silicon is available to the fungus from the host, deposition or an active polymerization process must occur specifically in the membrane protrusions, HMC walls and septa as seen in the present study, and in the neck ring (9), but not elsewhere in the fungus. The mechanisms of silicon deposition in higher plants are still not clear, although many hypotheses, mainly attributing deposition to the impedance of the evapotranspiration stream, have been put forward (30–32). However, recent evidence indicates that metabolic activity of some kind may also be involved in the formation of silicon deposits (18). Also, a metabolic role for silicon in the germination of *Erysiphe graminis hordei* conidia was indicated (23). The specificity of the occurrence of silicon in the haustorial apparatus observed in the present study and elsewhere (9) further indicates a controlled metabolic deposition of silicon. These results also demonstrate the importance of individual cell orientation in structural studies of host-rust fungal interactions. The observed responses may vary depending on the location of the observed host cell within the region of the colony and the time of infection.

Polyphosphates (or inorganic phosphates) have been reported in a number of organisms including several fungi (3,34). Characteristically, all of these inclusions were detected within vacuoles (6,34). It is probable that the phosphorous-rich sulphur and iron-containing deposits found in the HMCs and haustoria of *P. coronata avenae* as determined by our EDX analysis were analogous to the inorganic phosphates reported above. In the vesicular-arbuscular mycorrhizal system it was suggested that phosphates were taken up by the fungus from the soil, and after conversion, polyphosphates were translocated as vacuolar granules to active arbuscules (7). By analogy, it may be that phosphates were taken up by the haustoria of *P. coronata avenae* from host cells and after conversion, polyphosphates were then translocated to other parts of the mycelium. This is consistent with the finding that much of the polyphosphate found in *P. graminis tritici* was located in the urediospores (3) and the only source of phosphates was from the host.

Nishi (27) has reported that a large amount of polyphosphate in the spores of *Aspergillus niger* was utilized during germination. A similar observation was made in the germinating urediospores of *P. graminis tritici* (3). At present, a number of functions have been proposed for polyphosphate (6,15). Polyphosphate accumulation is a mechanism for regulating orthophosphate levels in some cells and as well could be an energy storage mechanism. Such accumulation also allows large amounts of phosphorus to be stored in a "nonleaking" form (13). Any of these possible roles may be applicable to *P. coronata avenae*.

Electron-opaque deposits were frequently detected in the vacuoles of hyphal cells and in the small vacuoles of young HMCs of *P. coronata avenae*. These vacuolar deposits were found in stained sections of glutaraldehyde/OsO_4-fixed material, but it is not certain if they are analogous to the unstained, unosmicated electron-opaque deposits revealed in older HMCs and haustoria by EDX analysis. Similar vacuolar electron-opaque deposits were reported in germinating urediospores, appressoria, and substomatal vesicles, but not in the elongating germ tubes nor in the vacuolating HMCs of *U. phaseoli vignae* (20). The vacuolar electron-opaque deposits in *U. phaseoli vignae* were also found in stained sections of glutaraldehyde/OsO_4-fixed material, and there was no evidence of phosphorus after EDX analysis of the deposits

(20). Certain elements, including phosphorus, are extractable by OsO_4 (25). Possibly the absence of phosphorus in the vacuolar deposits in *U. phaseoli vignae* resulted from OsO_4 extraction. However, if the commonly observed vacuolar deposits in the young HMCs of *P. coronata avenae* should prove to be polyphosphates, this would implicate the involvement of polyphosphates in haustorium formation. This is not unreasonable because large amounts of both energy and phosphorus would be required for the synthesis of at least phospholipids during haustorium formation.

LITERATURE CITED

1. Allen, R. F. 1923. Cytological studies of infection of Baart, Kanred and Mindum wheats by *Puccinia graminis tritici* forms III and XIX. J. Agric. Res. 26:571-604.
2. Bartnicki-Garcia, S. 1968. Cell wall chemistry, morphogenesis and taxonomy of fungi. Annu. Rev. Microbiol. 22:87-108.
3. Bennett, J., and Scott, K. J. 1971. Inorganic polyphosphates in the wheat stem rust fungus and in rust-infected wheat leaves. Physiol. Plant Pathol. 1:185-198.
4. Boer, P. 1979. Glycosylation of yeast and fungal cell wall components. Biochem. Soc. Trans. 7:331-333.
5. Bracker, C. E., and Littlefield, L. J. 1973. Structural concepts of host-pathogen interfaces. Pages 159–318 in: Fungal Pathogenicity and the Plant's Response. R. J. W. Byrde and C. V. Cutting, eds. Academic Press, London. 499 pp.
6. Bullock, S., Ashford, A. E., and Willets, H. J. 1980. The structure and histochemistry of sclerotia of *Sclerotinia minor* Jagger. II. Histochemistry of extracellular substances and cytoplasmic reserves. Protoplasma 104:333-351.
7. Callow, J. A., Capaccio, L. C. M., Parish, G., and Tinker, P. B. 1978. Detection and estimation of polyphosphate in vesicular-arbuscular mycorrhizas. New Phytol. 80:125-134.
8. Chong, J. 1981. Ontogeny of mono- and dikaryotic haustoria of *Puccinia coronata avenae*: Ultrastructure, cytochemistry and electron-probe X-ray analysis. Ph.D. thesis. University of Manitoba, Winnipeg, Canada. 169 pp.
9. Chong, J., and Harder, D. E. 1980. Ultrastructure of haustorium development in *Puccinia coronata avenae*. I. Cytochemistry and electron probe X-ray analysis of the haustorial neck ring. Can. J. Bot. 58:2496-2505.
10. Chong, J., Harder, D. E., and Rohringer, R. 1981. Ontogeny of mono- and dikaryotic rust haustoria: Cytochemical and ultrastructural studies. Phytopathology 71:975-983.
11. Courtoy, R., and Simar, L. J. 1974. Importance of controls for the demonstration of carbohydrates in electron microscopy with the silver methenamine or the thiocarbohydrazide-silver proteinate method. J. Microsc. (Oxf.) 100:199-211.
12. Craig, A. S. 1974. Sodium borohydride as an aldehyde-blocking reagent for electron microscope histochemistry. Histochemistry 42:141-144.
13. Farrar, J. F. 1976. The uptake and metabolism of phosphate by the lichen *Hypogymnia physodes*. New Phytol. 77:127-134.
14. Hall, J. L. 1978. Electron microscopy and cytochemistry of plant cells. Biomedical Press, New York. 444 pp.
15. Harold, F. M. 1966. Inorganic polyphosphates in biology: Structure, metabolism, and function. Bacteriol. Rev. 30:772-794.
16. Hayat, M. A. 1975. Positive staining for electron microscopy. Van Nostrand Reinhold Company. New York. 361 pp.
17. Heath, M. C. 1974. Light and electron microscope studies of the interactions of host and non-host plants with cowpea rust, *Uromyces phaseoli* var. *vignae*. Physiol. Plant Pathol. 4:403-414.
18. Heath, M. C. 1979. Partial characterization of the electron-opaque deposits formed in the non-host plant, French bean, after cowpea rust infection. Physiol. Plant Pathol. 15:141-148.
19. Heath, M. C., and Heath, I. B. 1975. Ultrastructural changes associated with the haustorial mother cell during haustorium formation in *Uromyces phaseoli* var. *vignae*. Protoplasma 84:297-314.
20. Heath, I. B., and Heath, M. C. 1979. Structural studies of the development of infection structures of cowpea rust, *Uromyces phaseoli* var. *vignae*. II. Vacuoles. Can. J. Bot. 57:1830-1837.
21. Hickey, E. L., and Coffey, M. D. 1978. A cytochemical investigation of the host-parasite interface in *Pisum sativum* infected by the downy mildew fungus *Peronospora pisi*. Protoplasma 97:201-220.
22. Hunsley, D., and Burnett, J. H. 1970. The ultrastructural architecture of the walls of some hyphal fungi. J. Gen. Microbiol. 62:203-218.
23. Kunoh, H., Takamatsu, S., and Ishizaki, H. 1978. Cytological studies of early stages of powdery mildew in barley and wheat. III. Distributions of residual calcium and silicon in germinated conidia of *Erysiphe graminis hordei*. Physiol. Plant Pathol. 13:319-325.
24. Littlefield, L. J., and Heath, M. C. 1979. Ultrastructure of Rust Fungi. Academic Press, New York, San Francisco, London. 277 pp.
25. Lott, J. N. A., Greenwood, J. S., and Vollmer, C. M. 1978. An energy dispersive X-ray analysis study of elemental loss from globoid crystals in protein bodies as a result of osmium tetroxide fixation. Can. J. Bot. 56:2408-2414.
26. Nagahashi, G., Leonard, R. T., and Thomson, W. W. 1978. Purification of plasma membranes from roots of barley. Specificity of the phosphotungstic acid-chromic acid stain. Plant Physiol. 61:993-999.
27. Nishi, A. 1961. Role of polyphosphate and phospholipid in germinating spores of *Aspergillus niger*. J. Bacteriol. 81:10-19.
28. Ruttle, M. L., and Fraser, W. P. 1927. A cytological study of *Puccinia coronata* Cda. on Banner and Cowra 35 oats. Univ. Calif. Publ. Bot. 14:21-72.
29. Samborski, D. J., Kim, W. K., Rohringer, R., Howes, N. K., and Baker, R. J. 1977. Histological studies on host-cell necrosis conditioned by the Sr6 gene for resistance in wheat to stem rust. Can. J. Bot. 55:1445-1452.
30. Sangster, A. G., and Parry, D. W. 1976. Endodermal silicification in mature nodal roots of *Sorghum bicolor* (L.) Moench. Ann. Bot. (Lond.) 40:373-379.
31. Sargent, P., and Gay, J. L. 1977. Barley epidermal apoplast structure and modification by powdery mildew contact. Physiol. Plant Pathol. 11:195-205.
32. Scurfield, G., Anderson, C. A., and Segnit, E. R. 1974. Silica in woody stems. Aust. J. Bot. 22:211-219.
33. Thiéry, J. P. 1967. Mise en évidence des polysaccharides sur coupes fines en microscopie électronique. J. Microsc. (Paris). 6:987-1018.
34. White, J. A., and Brown, M. F. 1979. Ultrastructure and X-ray analysis of phosphorus granules in a vesicular-arbuscular mycorrhizal fungus. Can. J. Bot. 57:2812-2818.